

Articles

Spectroscopic Studies on the High- T_c Superconducting $\text{La}_2\text{CuO}_{4+\delta}$ Prepared by Electrochemical Oxidation

Jung-Chul Park*, Alain Wattiaux**, Jean-Claude Grenier**, Dong-Hoon Kim†, and Jin-Ho Choy†

*Department of Chemistry, College of Natural Sciences, Pusan Women's University, Pusan 617-736, Korea

**Institut de Chimie de la Matière Condensée de Bordeaux du CNRS, Université Bordeaux I, 33600 Pessac Cedex, France

†Center for Molecular Catalysis (CMC), Department of Chemistry, College of Natural Sciences,

Seoul National University, Seoul 151-742, Korea

Received August 8, 1996

A superconducting phase $\text{La}_2\text{CuO}_{4+\delta}$ ($T_c=44$ K) has been prepared by electrochemical oxidation which allows the oxygen to intercalate into the La_2O_2 layers. According to the Cu K-edge X-ray absorption near edge structure spectroscopic analysis, the oxidized phase shows an overall spectra shift of about 0.5 eV to a higher energy region compared to the as sintered one with the occurrence of an additional peak corresponding to the transition to the $|1s^13d^{n+1}L^{-1}4p\sigma^1\rangle$ final state, indicating the oxidation of CuO_2 layer. From the X-ray photoelectron spectroscopic studies, it is found that the binding energy of La $3d_{5/2}$ is significantly shifted from 834.3 eV (as sintered La_2CuO_4) to 833.6 eV (as electrochemically oxidized $\text{La}_2\text{CuO}_{4+\delta}$), implying that the covalency of the (La-O) bond is decreased due to the oxygen intercalation. The O 1s spectra do not provide an evidence of the superoxide or peroxide, but the oxide (O^{2-}) with the contaminated carbonate (CO_3^{2-}) based on the peaks at 529 eV and 532 eV, respectively, which is clearly confirmed by the Auger spectroscopic analysis. Oxygen contents determined by iodometric titration ($\delta=0.07$) and thermogravimetry ($\delta=0.09$) show good coincidence each other, also giving an evidence for the " O^{2-} " nature of excess oxygen. From the above results, it is concluded that " O^{2-} " appeared as O 1s peak at 528.6 eV is responsible for superconductivity of $\text{La}_2\text{CuO}_{4+\delta}$.

Introduction

The undoped La_2CuO_4 shows the filamentary superconductivity¹ and, after the treatment such as high oxygen pressure annealing or chimie douce (soft chemistry) reaction, it becomes superconducting with T_c between 30 and 44 K.^{2,3} Thanks to the intensive studies on this superconducting system, it is now widely accepted that the formation of Cu^{3+} ion makes a crucial role for the superconductivity.^{4,5} On the other hand, the nature of the counter anion, namely, excess oxygen is still ambiguous for the present. Schirber *et al.*⁶ reported that the excess oxygen species in $\text{La}_2\text{CuO}_{4+\delta}$ are intercalated as the superoxide, O_2^- , on the basis of thermogravimetric analysis ($\delta=0.13$) and iodometric titration ($\delta=0.032$). Subsequently, the above argument was supported by Rogers *et al.*⁷ using X-ray photoelectron spectroscopy (XPS). On the contrary, there were some papers against the identification of superoxide ion in $\text{La}_2\text{CuO}_{4+\delta}$. Zhou *et al.*⁸ pointed out that in $\text{La}_2\text{CuO}_{4+\delta}$ ($\delta=0.05$), the type of excess oxygen responsible for superconductivity is not superoxide ion, but " O^{2-} ". Also, XPS study of the oxygen enriched $\text{La}_2\text{CuO}_{4+\delta}$ ($\delta=0.03$) was carried out by Strongin *et al.*⁹ who indicated only a single peak at 529 eV without any evidence of superoxide ion in the lattice.

Some problems for identifying the nature of excess oxygen may arise due to an intrinsic small oxygen content as well as analytical tools such as surface-sensitive XPS, iodometric titration, and thermogravimetric analysis (TGA).

According to the TG thermograms and magnetic data reported previously,¹⁰ the deintercalation reaction of excess ox-

xygen occurs between 80 °C and 250 °C. Physically adsorbed species, such as hydroxyl groups, water molecules and carbon related molecules, result in a considerable weight-loss in TGA. Since the binding energies of the O 1s electron of physically adsorbed species (OH groups, H_2O , carbon-related molecules, etc.) are very similar to one another, the loss may give rise to a serious misinterpretation of the XPS spectra. It is, therefore, difficult to interpret the nature of excess oxygen appeared in the XPS spectra of $\text{La}_2\text{CuO}_{4+\delta}$ ($\delta=0.03$, with very small oxygen content) whether they are oxide (O^{2-}), peroxide (O_2^{2-}), or superoxide ions (O_2^-).

Recently, Grenier *et al.* have proposed the oxygen diffusion model in electrochemical oxidation based on the reversible electron transfer between metal and oxygen.¹¹ In the hypothesis, they argued that an oxide ion adsorbed on the electrode surface gives an electron to the metal cation and transforms to a peroxide one during the diffusion process. This peroxide recovers its electron after the diffusion and is stabilized as an oxide species in the lattice.

In the present paper, spectroscopic evidences for the above suggestion based upon XPS and X-ray absorption near edge structure (XANES) of the $\text{La}_2\text{CuO}_{4+\delta}$ produced by an electrochemical oxidation will be discussed with TGA, iodometric titration, and Auger emission spectroscopy (AES) in order to elucidate the chemical nature of excess oxygen.

Experimental

The La_2CuO_4 has been prepared by conventional solid

state reaction from a stoichiometric mixture of dried La₂O₃ and CuO which are heated in air at 1050 °C for 18 hrs, sintered in air at 1050 °C for 16 hrs and then quenched. Experimental conditions of the electrochemical oxidation for La₂CuO₄ have been previously described.^{10,12} Sintered disk (8 mm in diameter, ~2 mm in thickness) of the pristine La₂CuO₄ was used as a working electrode. The pellet was attached to copper rod with silver paste, then the rod and the Teflon cast was filled with the insulating Epoxy resin to protect the rod from the electrolyte (1 N KOH).

This working electrode was placed at the center of the larger vessel in two-compartment cell. Hg/HgO reference electrode (*E* vs. SHE=+98 mV at pH 14) was then placed near the working electrode. Pt coil used as a counter electrode was placed in the smaller vessel of the reaction cell. Electrochemical oxidation was carried out at room temperature under air by applying constant potential of +450 mV (vs. Hg/HgO electrode).

The elemental analysis of La and Cu was achieved by inductively coupled plasma-emission spectroscopy (ICP) with a Labtam 8400 spectrometer, and the oxygen content was estimated, assuming O²⁻ species, from the value of the Cu³⁺/Cu²⁺ ratio, which was determined by the iodometric titration.¹³ In order to estimate the oxygen content, TGA (Setaram thermobalance MTB-10-8 model) was also performed with a heating rate of 1 °C/min under Ar atmosphere (flow rate=5 ml/min).

Electrical resistivity measurements were performed by using conventional four probe method with temperature range from room temperature to 10 K. The variation of magnetization and magnetic susceptibility as a function of applied magnetic field and of temperature were examined by a FONER type vibrating sample magnetometer.

X-ray photoelectron spectra were recorded as a function of sputtering time on a PHI 5100 Perkin-Elmer spectrometer (resolution: ±0.2 eV). Unmonochromatized Mg-K_α radiation of 1253.6 eV was used and the base pressure in the spectrometer was in the order of 2.0×10⁻¹⁰ torr. The binding energies were corrected from the known reference (binding energy of C 1s: 284.6 eV). Auger emission spectra were registered with the excitation source of 3 keV using Physical Electronics 590.

The X-ray absorption spectroscopic measurements have been carried out at the beam line of BL7C and 10B in Photon Factory at Tsukuba, Japan, running at 2.5 GeV with a stored current of ca. 300-360 mA. Samples were ground to fine powders in a mortar with nujol as a diluent, and then spread uniformly onto an adhesive tape, which was folded into some layers to obtain an optimum absorption jump ($\Delta\mu \approx 1$) enough to be free from the thickness and pin-hole effects.

Results and Discussion

Electrochemical oxidation. The electrochemical behavior of La₂CuO₄ in 1 N KOH solution, in the potential range 200≤*E*≤800 mV, shows an oxidation plateau A (arrow A in Figure 1) between 600 and 800 mV just before the oxygen evolution.

The potentials may correspond, in the potential-pH diagram of copper,¹⁴ to those of possible theoretical equilibria

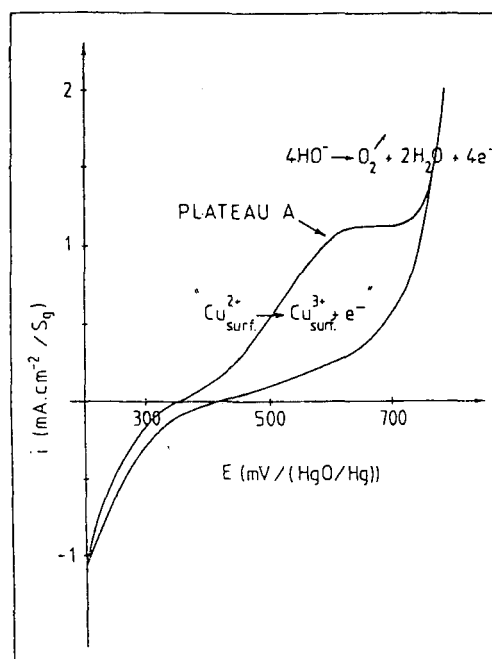


Figure 1. Cyclic voltammogram for La₂CuO₄ in 1 N KOH (6 mVs⁻¹).

which are concerned with hydrated oxide of oxyhydroxides of Cu^{II}, Cu^{III} or even Cu^{IV}. However, the latter with such a high oxidation state is doubtful. A study as a function of potential and various sweep rates has shown that the best condition for oxidizing this material was 450 mV.

The potential value at *i*=0 (*E*_{*i*=0}) measured before polarization (350 mV) increases up to 400 mV after the polarization. As this potential is correlated both to the involved redox couple and to the value of the Fermi level energy of the material, this change implies at least a noticeable modification of its surface.

Physicochemical characterization. In oxygen evolution reaction, it is well known that OH⁻ ions in alkaline electrolyte are adsorbed on the electrode surface (or metal oxide surface), and continuously transformed into the type of (O)_{ads}, which finally followed by the oxygen evolution through an electron transfer step.¹⁵

So, the oxygen species may gradually diffuse into the La₂CuO₄ lattice and at the same time, the transition metal ions (here, Cu²⁺) are oxidized to a higher valent state. Based on the oxidation phenomena, we performed electrochemical treatments at an applied potential of 450 mV before oxygen evolution.

After electrochemical oxidation of the La₂CuO₄ pellet, it was cleaned with distilled water and absolute alcohol, dried, and then characterized. The refined unit cell parameters determined from XRD patterns as shown in Figure 2 are as follows:

- i) before oxidation; *a*=5.352 Å, *b*=5.405 Å, and *c*=13.154 Å
- ii) after oxidation; *a*=5.351 Å, *b*=5.420 Å, and *c*=13.227 Å.

As shown in Figure 2, La₂CuO₄ after oxidation exhibits an enhanced orthorhombic distortion with an expansion of unit cell volume ($\Delta V/V=0.8\%$) mainly due to the increase of *c* parameter. The distortion implies that some oxygens are introduced into the La₂CuO₄ lattice during electrochemical

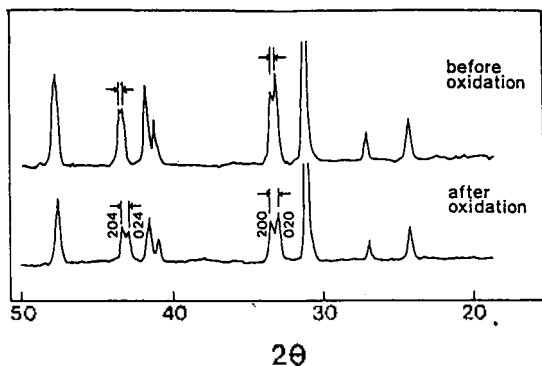


Figure 2. X-ray diffraction patterns of La_2CuO_4 before and after electrochemical oxidation.

oxidation.

After oxidation, the electrical resistivity was measured as a function of pellet thickness in order to examine whether our electrochemical treatment is only a simple surface oxidation technique or not. For this treatment, a dense La_2CuO_4 ceramic with about 90% of theoretical density ($\phi \cong 8$ mm, $h \cong 2$ mm) has been embedded in epoxy resin and polished. After electrochemical treatment, the temperature dependent electrical resistivity has been measured for the La_2CuO_4 ceramic ground with sand paper. As presented in Figure 3, approaching to the electrode surface which was supposed to be more exposed to electrolyte (1 N KOH), the electrical resistivity becomes lower. Finally the lowest resistivity, which is the same as that of electrode surface, is observed at $t=1.0$ mm measured from the pellet surface ($T_{c,on-set}=50$ K, $T_{c,off-set}=44$ K).

The result indicates that the electrochemical oxidation allows the La_2CuO_4 ceramic to oxidize not only at the surface, but also in the bulk. Thus, the oxidized species diffuse gra-

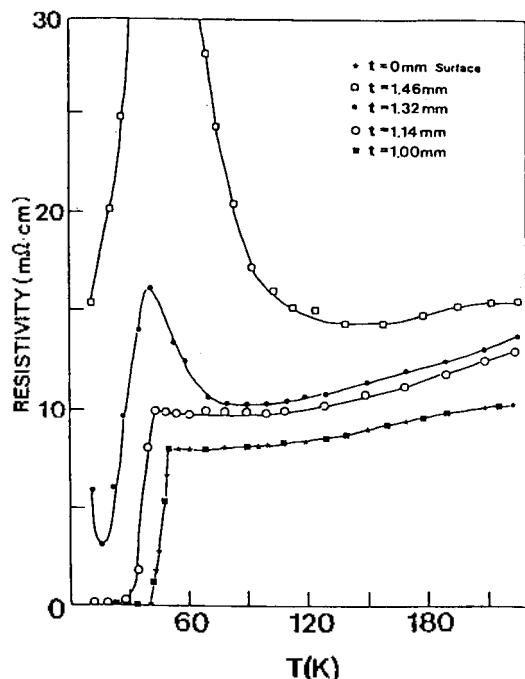


Figure 3. The electrical resistivity as a function of pellet thickness for $\text{La}_2\text{CuO}_{4+\delta}$.

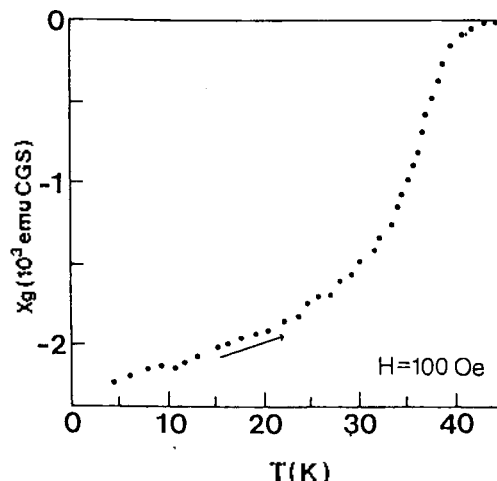


Figure 4. Temperature dependence of the diamagnetic susceptibility of $\text{La}_2\text{CuO}_{4.48}$ after electrochemical oxidation.

dually into the bulk of ceramic during electrochemical oxidation.

The magnetic susceptibility value measured under a magnetic field of 100 Oe becomes negative below 44 K (Figure 4), which is consistent with the resistivity data.

The La/Cu ratio in the starting material La_2CuO_4 is estimated as a stoichiometric one ($\text{La}/\text{Cu}=2.00 \pm 0.01$) using ICP. The oxygen contents determined by iodometric titration are as follows:

- i) Before oxidation; $\text{La}_2\text{CuO}_{4.00 \pm 0.01}$
- ii) After oxidation; $\text{La}_2\text{CuO}_{4.07 \pm 0.01}$

Figure 5 represents TG thermograms performed under the same conditions for three pellets. The curve (I) was obtained from La_2CuO_4 after electrochemical treatment, and the curve (II) after immersion in the electrolyte without an applied potential. It is worthy to note here that the X-ray diffraction pattern and the electrical resistivity of La_2CuO_4 after immersion in 1 N KOH solution were not changed as the starting material. The curve (III) corresponds to the starting

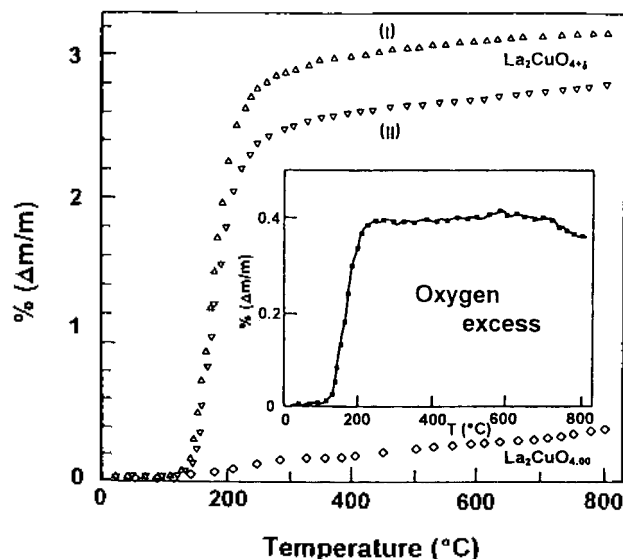


Figure 5. The excess oxygen content in $\text{La}_2\text{CuO}_{4.48}$.

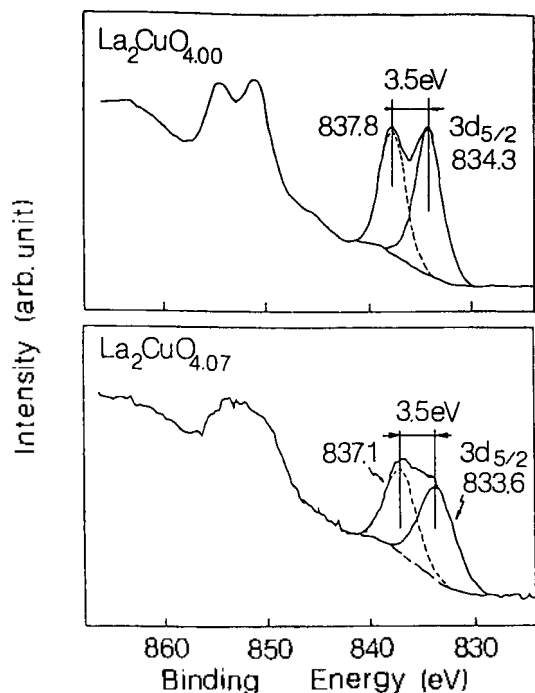


Figure 6. La(3d) XPS spectra of $\text{La}_2\text{CuO}_{4.0}$ before and after electrochemical oxidation.

material $\text{La}_2\text{CuO}_{4.0}$. The difference between curves (I) and (II) is given in the inset of Figure 5.

The weight loss begins below 100 °C, and remains constant around 250 °C.

The excess oxygen corresponds to $\delta \approx 0.09$ which is in good agreement with the value of iodometric titration ($\delta \approx 0.07$).

Such a good coincidence between iodometric titration and thermogravimetric analysis implies that the nature of excess oxygen is mainly "O²⁻".

XPS and XANES analyses. Figure 6 represents the La 3d core level binding energy for La_2CuO_4 before and after electrochemical oxidation. After curve fitting, the La 3d_{5/2} peak for the oxidized $\text{La}_2\text{CuO}_{4.07}$ appears to be shifted to the lower energy side by about 0.7 eV than that of the pristine La_2CuO_4 (before oxidation).

As Chaillout *et al.* reported previously,¹⁶ since excess oxygens are introduced into the La_2O_2 planes, and the coordination number of La increases from 9 to 10, the covalency of the (La-O) bond decreases with an increase of bond distance. Therefore, the binding energy of La 3d_{5/2} becomes smaller after electrochemical oxidation.

However, the Cu 2p binding energy shifts could not be observed after electrochemical oxidation as shown in Figure 7. In X-ray photoelectron spectra of LaCuO_3 ,¹⁷ the binding energy of Cu 2P_{3/2} is shifted 2.5 eV to higher energy side compared to La_2CuO_4 . Since the increase of Cu³⁺ content after electrochemical oxidation was only about 14% as determined by the iodometric titration, no considerable chemical shift was observed within the resolution range of spectrophotometer (≈ 0.2 eV).

In order to solve this problem, we have performed the Cu K-edge X-ray absorption spectroscopic analysis for La_2CuO_4 before and after electrochemical oxidation because the fine

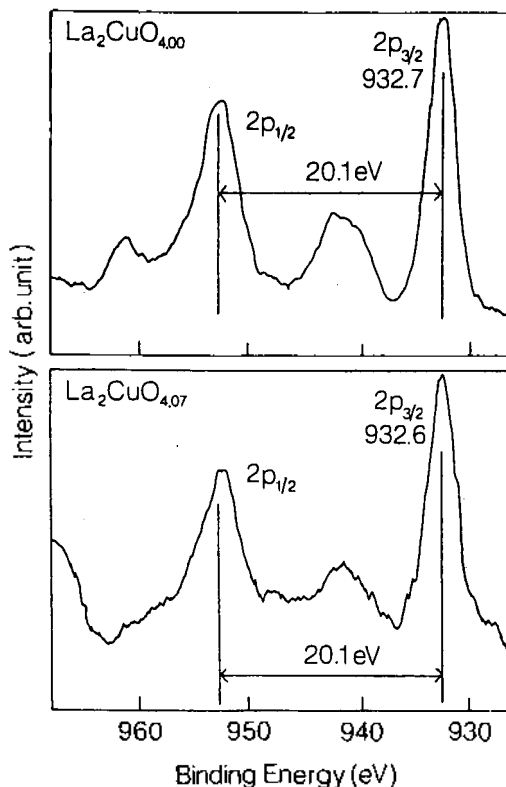


Figure 7. Cu(2p) XPS spectra of $\text{La}_2\text{CuO}_{4.0}$ before and after electrochemical oxidation.

spectral features in XANES region could provide an information even on the small modification of electronic and geometric structures. Figure 8 shows the Cu K-edge XANES spectra and their second derivatives of the pristine La_2CuO_4 and the electrochemically oxidized $\text{La}_2\text{CuO}_{4.07}$, together with the divalent and trivalent copper oxide references of Nd_2CuO_4 , LaCuO_3 , and $\text{La}_7\text{Li}_{0.5}\text{Cu}_{0.5}\text{O}_4$ for comparison.

It is worthy to note here that there is an overall peak shift of about 0.5 eV to a higher energy region in the spectrum after electrochemical oxidation, indicating the enhancement of oxidation state of CuO₂ layer. The electrochemical oxidation has a more remarkable effect on the fine spectral features. As shown in Figure 8b, the spectrum of $\text{La}_2\text{CuO}_{4.07}$ exhibits an additional peak A' which is absent in that of La_2CuO_4 . According to the previous X-ray absorption spectroscopic study,⁵ the split peaks of A and A' correspond to the transitions to the $[\text{1s}^1\text{3d}^{n-1}\text{L}^1\text{4p}\pi^1]$ final state and to the $[\text{1s}^1\text{3d}^{n-1}\text{L}^1\text{4p}\sigma^1]$ one accompanied by shakedown process, respectively. Although the former transition through π -bonding channel occurs generally for most of divalent copper ion, the latter one along the σ -bonding is not allowed due to the strong electrostatic repulsion with in-plane oxygen ligands.

For this reason, the peak A' corresponding to the transition to $[\text{1s}^1\text{3d}^{n-1}\text{L}^1\text{4p}\sigma^1]$ is not observed for all the present divalent reference spectra of Nd_2CuO_4 and La_2CuO_4 . However, in case of $\text{La}_2\text{Li}_{0.5}\text{Cu}_{0.5}\text{O}_4$ with trivalent copper, the shakedown process along the σ bonding as well as along the π bonding is allowed since the increase of copper valence makes the charge transfer from oxygen ligand to

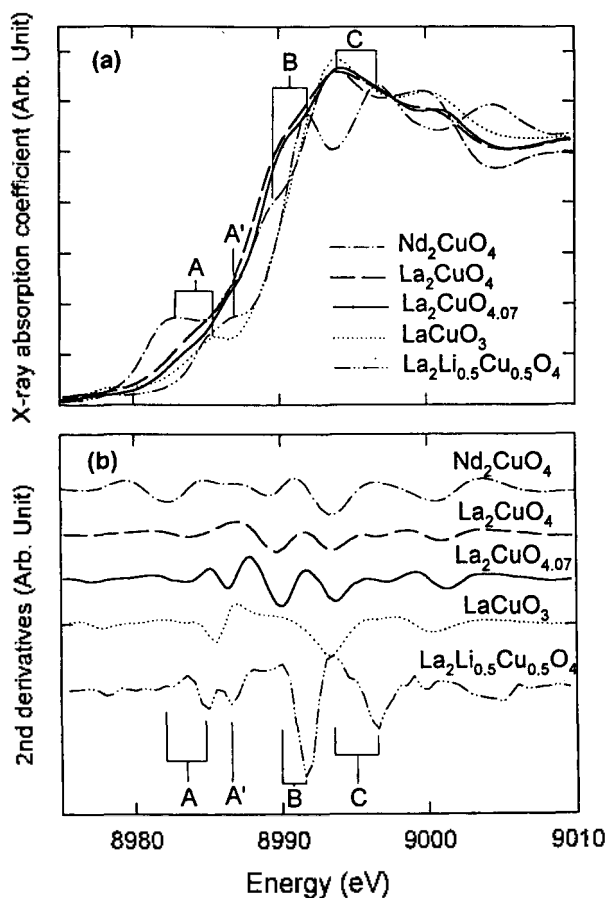


Figure 8. Cu K-edge XANES (a) spline and (b) second derivative spectra of La_2CuO_4 before and after electrochemical oxidation, together with the reference spectra of Nd_2CuO_4 , LaCuO_3 , and $\text{La}_2\text{Li}_{0.5}\text{Cu}_{0.5}\text{O}_4$.

copper electrostatically favorable. In this respect, the occurrence of the peak A' in the spectrum of $\text{La}_2\text{CuO}_{4.07}$ provides an evidence on the partial formation of Cu^{III} ion upon electrochemical oxidation, indicating the oxidation of CuO_2 layer.

The binding energies of O 1s were assigned after curve-fitting (Figure 9). Particularly, after electrochemical oxidation, the O 1s binding energy of 532.4 eV was found to be very similar to that of 532.1 eV observed by Rogers *et al.*⁷ They interpreted that such a high binding energy is appreciably correlated with the contaminated species in the near-surface region of the La_2CuO_4 ceramic even in the blank sample. They also attempted to remove the carbonated species by annealing the samples at 925 K for 24 hrs. However, we think it is not sufficient to remove the carbonated species completely under their annealing conditions. Reversely, Strongin *et al.*⁹ pointed out that the O 1s peak at 532.2 eV was nearly removed by surface scraping in the $\text{La}_2\text{CuO}_{4.5}$ ceramic, and they obtained only a single peak at 529 eV corresponding to " O^{2-} ". In our experiment, however, both the carbonated species and the hydroxyl one can be introduced into the bulk through open pores and grain boundaries of the ceramic sample during electrochemical oxidation in an aerated KOH solution. Auger emission spectroscopic analysis confirms the presence of carbonated species which appeared at 532.4 eV in X-ray photoelectron

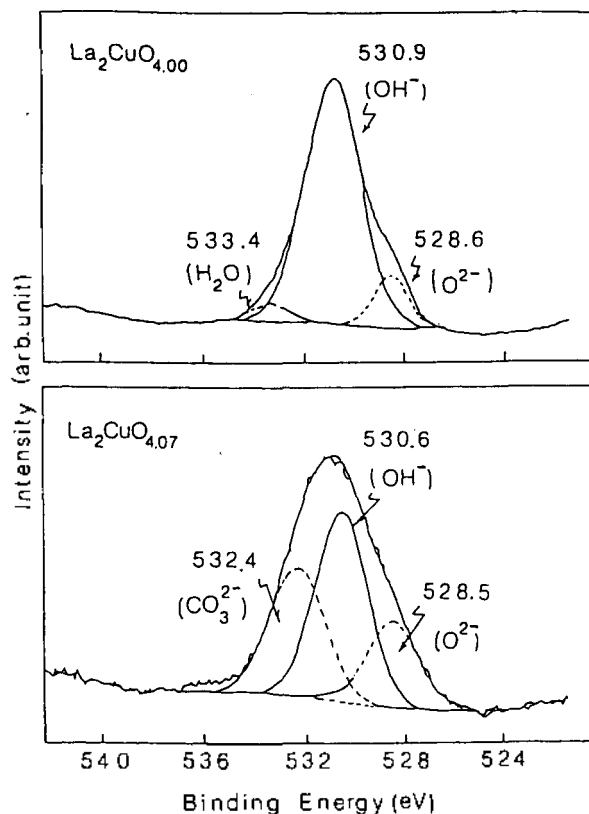


Figure 9. O(1s) XPS spectra of $\text{La}_2\text{CuO}_{4.07}$ before and after electrochemical oxidation.

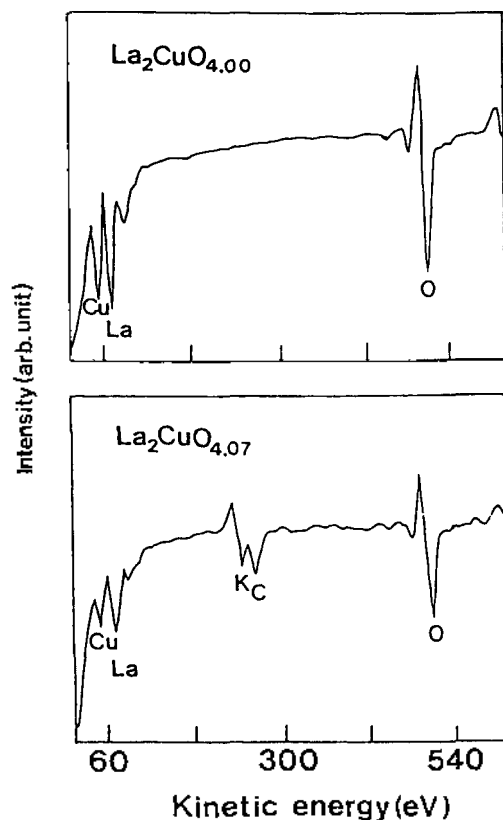


Figure 10. Auger emission spectra of $\text{La}_2\text{CuO}_{4+\delta}$ ($\delta=0$ and 0.07).

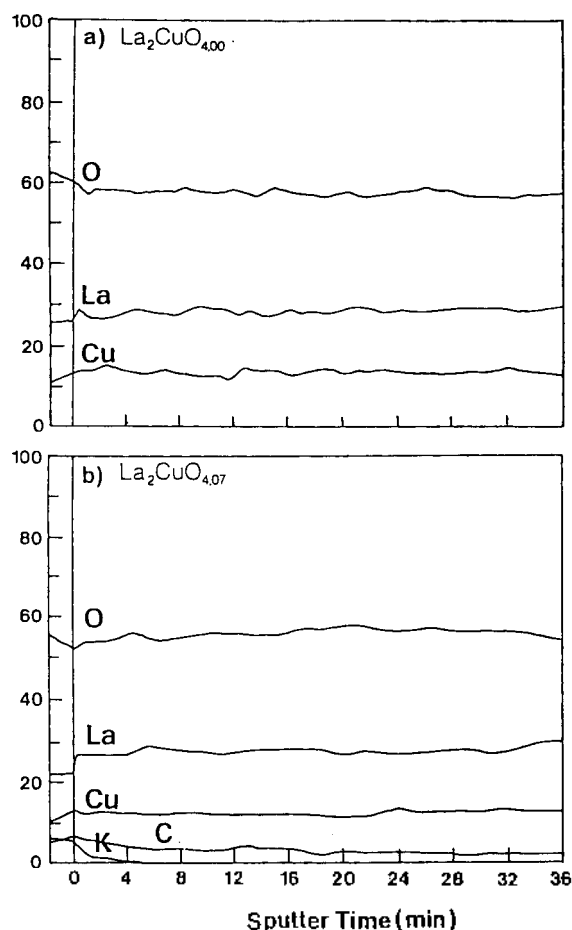


Figure 11. Atomic percentage of $\text{La}_2\text{CuO}_{4.5}$ before and after electrochemical oxidation.

spectra of the electrochemically oxidized $\text{La}_2\text{CuO}_{4.5}$ ceramic.

As shown in Figure 10, it is clearly seen that new Auger lines corresponding to potassium and carbon were appeared after electrochemical oxidation in an aerated KOH solution. As the Auger emission spectroscopy is highly dependent on surface matrix effects, the depth profile is necessary to examine the presence of contaminated layers.

Figure 11 shows the atomic percentage of La_2CuO_4 materials before and after electrochemical oxidation. The atomic percentages (La, Cu, and O) of La_2CuO_4 materials are nearly constant even after Ar-ion sputtering (250 Å/min). In particular, the percentages of potassium and carbon atoms produced during electrochemical oxidation are only slightly decreased despite of the prolonged sputtering time. This experimental evidence is clearly consistent with the O 1s binding energy of 532.4 eV, which is originated from the carbonated species contaminated during electrochemical oxidation as shown in Figure 10.

According to the thermal evolution of magnetic susceptibility of La_2CuO_4 before and after oxidation at $T > T_c$, as represented in Figure 12, it shows the Pauli-type paramagnetization after oxidation, which is well consistent with the enhanced metallic character.

From the above findings, it is concluded that the nature of excess oxygen stabilized in electrochemically produced $\text{La}_2\text{CuO}_{4.5}$ lattice is oxide ion, " O^{2-} ". No evidence for the

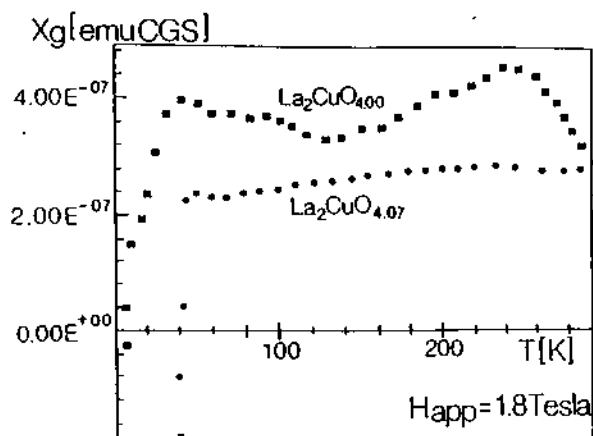


Figure 12. Thermal evolution of magnetic susceptibility of $\text{La}_2\text{CuO}_{4.5}$ at $T > T_c$.

formation of peroxide or superoxide can be found. It is also certain that O^{2-} appeared as the O 1s peak at 528.6 eV gives rise to the partial formation of Cu^{3+} , which is responsible for the superconductivity of $\text{La}_2\text{CuO}_{4.5}$.

Acknowledgment. This work was supported by NON DIRECTED RESEARCH FUND, Korea Research Foundation (1995). The authors are grateful to Prof. M. Nomura in Photon Factory for supporting the synchrotron radiation experiments.

References

- Grant, P. M.; Parkin, S. S. P.; Lee, V. Y.; Engler, E. M.; Ramirez, M. L.; Lim, G.; Jacowitz, R. D. *Phys. Rev. Lett.* **1987**, *58*, 2482.
- Beille, J.; Cabanel, R.; Chailout, C.; Chevalier, B.; Demazeau, G.; Deslands, F.; Etourneau, J.; Lejay, P.; Michel, C.; Provost, J.; Raveau, B.; Sulpice, A.; Tholence, J. L.; Tourmier, R. C. *R. Acad. Sci. Ser. 2* **1987**, *304*, 1097.
- Wattiaux, A.; Park, J.-C.; Grenier, J.-C.; Pouchard, M. *C. R. Acad. Sci. Ser. 2* **1990**, *310*, 1047.
- Choy, J.-H.; Kim, D.-K.; Hwang, S.-H.; Demazeau, G. *Phys. Rev. B* **1994**, *50*, 16631.
- Choy, J.-H.; Kim, D.-K.; Hwang, S.-H.; Park, J.-C. *J. Am. Chem. Soc.* **1995**, *117*, 7556.
- Schirber, J. E.; Morosin, B.; Merrill, R. M.; Hlava, P. F.; Venturini, E. L.; Kwak, J. F.; Nigrey, P. J.; Baughman, R. J.; Ginley, D. S. *Physica C* **1988**, *152*, 121.
- Rogers, Jr. J. W.; Shinn, N. D.; Schirer, J. E.; Venturini, E. L.; Ginley, D. S.; Morosin, B. *Phys. Rev. B* **1988**, *38*, 5021.
- Zhou, J.; Sinha, S.; Goodenough, J. B. *Phys. Rev. B* **1989**, *39*, 12331.
- Strongin, M.; Qiu, S. L.; Chen, J.; Lin, C. L.; McCarron, E. M. *Phys. Rev. B* **1990**, *41*, 7238.
- Park, J. C.; Huong, P. V.; Rey-Lafon, M.; Grenier, J. C.; Wattiaux, A.; Pouchard, M. *Physica C* **1991**, *177*, 487.
- Grenier, J.-C.; Pouchard, M.; Wattiaux, A. *Curr. Opin. Solid State & Mat. Sci.* **1996**, *1*, 233.
- Park, J. C.; Huong, P. V.; Grenier, J. C.; Wattiaux, A. J. *Less-Common Metals* **1990**, *164 & 165*, 862.

13. Choy, J. H.; Choi, S. Y.; Byeon, S. H.; Chun, S. H.; Hong, S. T.; Jung, D. Y.; Choe, W. Y.; Park, Y. W. *Bull. Korean Chem. Soc.* **1988**, *9*(5), 289.
14. Pourbaix, M. *Atlas d'équilibre électrochimique*; Gauthier-Villars: Paris (1963).
15. Mehandru, S. P.; Anderson, Alfred B. *J. Electrochem. Soc.* **1989**, *136*, 158.
16. Chaillout, C.; Cheong, S. W.; Fisk, Z.; Lehmann, M. S.; Marezio, M.; Morosin, B.; Schirber, J. E. *Physica C* **1989**, *158*, 183.
17. Allan, K.; Campion, A.; Zhou, J.; Goodenough, J. B. *Phys. Rev. B* **1990**, *41*, 11572.

Conformational Transition of Form II to Form I Poly(L-proline) and the Aggregation of Form I in the Transition: Water-Propanol Solvent System

Hyun Don Kim

Samsung Chemicals Technology Center (Samsung Advanced Institute of Technology),
103-6, Moonji-Dong, Yusong-Gu, Taejeon 305-380, Korea
Received February 11, 1997

The conformational transition of poly(L-proline) (PLP), Form II \rightarrow Form I and the intermolecular aggregation of the product, Form I, during and after the transition in water-propanol (1:7, 1:9, 1:15.7, and 1:29 v/v) were studied. For the study, the viscosity change and excess light scattering intensity were measured in the course of the transition which was determined by the Form I fraction, f_i of the sample solution. For the PLP sample of molecular weight $M_n=31,000$ the experimental results show that the reaction course is roughly divided into three regions: in the first region [$f_i=0.27$ to 0.40 ($-\alpha_D=400$ to 330)], the conformational change of Form II \rightarrow Form I occurs with decrease of viscosity, in the second region [$f_i=0.40$ to 0.80 ($-\alpha_D=330$ to 120)], a partial side-by-side (p-S-S) type aggregation in which Form I blocks interact with each other, which induces the increase of viscosity, starts to occur, and in the third region [$f_i=0.80$ to 1.00 ($-\alpha_D=120$ to 15)], a side-by-side type (raft like) aggregation of Form I or an end-to-end (E-E) type aggregation occurs according to the solvent situation, i.e., in a water-rich medium [water-propanol (1:9 or 1:7 v/v)], the (S-S) type aggregation with a gross decrease in viscosity occurs while in a water-poor medium [water-propanol (1:29 or 1:15.7 v/v)], the (E-E) type aggregation with a large increase in viscosity occurs. The (S-S) type aggregation was promoted at high temperatures. Based on the structure of PLP, a reasonable mechanism for the (p-S-S) and (S-S) aggregation which occurs with the transition of Form II \rightarrow Form I is considered. The suggested mechanism was also supported by the result of chain length effect of PLP for the aggregation.

Introduction

As well known, poly(L-proline) (PLP) is a polyimino acid polypeptide which, unlike poly- α -amino acid polypeptides, having no amide hydrogen (-NH), cannot form intermolecular hydrogen bonds and its compound distinctly existed as two helical forms, Form I and Form II, not only in the solution,¹⁻¹² but also in the solid state.¹³⁻¹⁵ Form I is a right-handed helix (RHH) (3.3 peptides per turn, 10_3) with all the peptide bonds in the *cis* conformation, and the Form II is a left-handed helix (LHH) (three peptide per turn, 3_1) with all the peptide bonds in the *trans* conformation. Structurally, Form I is more compact and rigid while Form II is comparatively extended. A reversible transition of Form I \rightleftharpoons (RHH) Form II (LHH) is induced by appropriate changes of the solvent conditions.¹⁻¹² Transition Form I \rightarrow Form II occurs in water and aliphatic acid, and its contrary transition occurs by the dilution of the water and aliphatic acid by 1-propanol (or 1-butanol) [e.g., water (acetic acid)-propanol (1:9 v/v, etc.)].

Particularly, Form II of PLP has been noted because of its similarity to fibrous protein, collagen which has proline as its second most abundant amino acid.

Even though many studies for the PLP compound, as mentioned in the above, have been conducted, no one has studied in detail on the aggregation phenomenon during the transition Form II \rightarrow Form I. Although it was true that the PLP aggregation phenomenon has been already noted for pure Form I,¹⁶ which is end product of the transition in acetic acid-propanol (1:3 v/v) and for pure Form II (in pure water),¹⁷⁻¹⁹ but it was not clarified the detailed mechanism (or structure) and the reason and also, they have not noted for the aggregation phenomenon which occurs during the transition of Form II \rightarrow Form I.

Many studies for intermolecular aggregation of helical polypeptides have been conducted.²⁰⁻²⁷ Two types of aggregation have been recognized: end-to-end (E-E) type and side-by-side (S-S) antiparallel type. The former type aggregation is formed through the end group interaction between amino and carbonyl residues at each of the helical ends,